HNUE JOURNAL OF SCIENCE
Natural Science, 2025, Volume 70, Issue 3, pp. 35-46
This paper is available online at http://hnuejs.edu.vn/ns
DOI: 10.18173/2354-1059.2025-0035

THE THERMODYNAMIC CONTACT ANGLE IN THE PREWETTING PHASE OF A BINARY BOSE-EINSTEIN CONDENSATE MIXTURE

Pham Duy Thanh* and Nguyen Van Thu
Faculty of Physics, Hanoi Pedagogical University 2, Phu Tho province, Vietnam
*Corresponding author: Pham Duy Thanh, e-mail: thanhdpham@outlook.com

Received August 2, 2025. Revised August 27, 2025. Accepted September 30, 2025.

Abstract. To investigate the prewetting state of a Bose-Einstein condensate (BEC) mixture adsorbed on an optical hard wall at zero temperature, we consider a system in which condensate 1 coexists with condensate 2 with the chemical potential held fixed. Using the double parabola approximation (DPA) and solving the coupled Gross-Pitaevskii equations, we derive an analytical expression for the thermodynamic contact angle based on Youngs equation. Although the resulting formula is not algebraically simple, it reveals that complete wetting can occur before the bulk coexistence point is reached, indicating the presence of a continuous (second-order) prewetting transition. Our findings are in agreement with theoretical predictions in the literature and emphasize that the wetting film thickness grows smoothly without a discontinuous jump. This work provides useful guidance for the design of experiments aimed at observing wetting phenomena in Bose-Einstein condensates.
Keywords: Bose-Einstein condensate, Gross-Pitaevskii theory, Prewetting phase transition, Thermodynamic contact angle.

1. Introduction

Wetting transitions in classical systems have long been understood within the framework of thermodynamic potentials and surface energies. However, their quantum analogs, particularly in dilute and weakly interacting Bose-condensed gas mixtures, remain less well explored. Of special interest is the behavior of BEC mixtures at optical hard walls, where surface effects play a crucial role in determining the equilibrium structure of the condensates. In this context, the concept of a thermodynamic contact angle emerges as a key quantity that characterizes the extent of wetting by one condensate phase in the presence of another.

In previous studies [1]-[4], the occurrence of wetting phase transitions in BEC mixtures confined by an optical wall has been theoretically proposed using the Gross-Pitaevskii (GP) mean-field framework at zero temperature. The phenomenon of wetting in binary BoseEinstein condensates (BECs) has been systematically investigated in a series of studies. Indekeu and Van Schaeybroeck (2004) first demonstrated the existence of an extraordinary wetting phase diagram, highlighting the transition from partial to complete wetting characterized by the thermodynamic contact angle [1]. This work was later extended by Van Schaeybroeck and Indekeu (2015), who provided a comprehensive analysis of wetting transitions, including critical wetting, first-order wetting, and prewetting phenomena, and constructed detailed phase diagrams to capture these behaviors [2]. Based on this foundation, Nguyen (2016) investigated the static properties of binary BEC mixtures confined by a hard wall within the GP framework, where the interfacial tension between the condensates and the phase boundary of the wetting transition were determined [3]. More recently, Pham and Nguyen (2024) extended this line of research to the prewetting phase, providing a quantitative identification of the nucleation line and the thickness of the prewetting layer [4], thereby refining the theoretical characterization of surface phase transitions in such systems.

However, none of the above studies have addressed the variation of the thermodynamic contact angle within the prewetting phase. Since the contact angle plays a central role in characterizing wetting and interfacial phenomena, understanding its behavior in the prewetting phase is essential for completing the theoretical picture of surface phase transitions in binary BEC mixtures. In this work, we aim to extend previous investigations by systematically analyzing the evolution of the contact angle along the prewetting line, thereby providing new insights into the interplay between film thickness, interfacial tension, and wetting transitions.

2. Content

2.1. Two-component BEC, wetting phase transition, coupled GP equations with a hard-wall condition

Figure 1 depicts a wetting transition in a two-component BEC, from a partially wetting configuration, which is defined by a finite thermodynamic contact angle θ (also known as the Young-Laplace angle), to a regime where θ approaches zero. In this limit, one component of the mixture, referred to as the wetting phase, forms a macroscopically thick layer that completely separates the other condensate from the wall, thus signaling the onset of complete wetting.

Let us denote the surface (free) energy per unit area of condensate j, $j = (1, 2)$, by γ_j, and the interfacial tension between the two condensates by γ_{12}. Under conditions of mechanical equilibrium at the three-phase contact line, Youngs law provides the following relation [7].

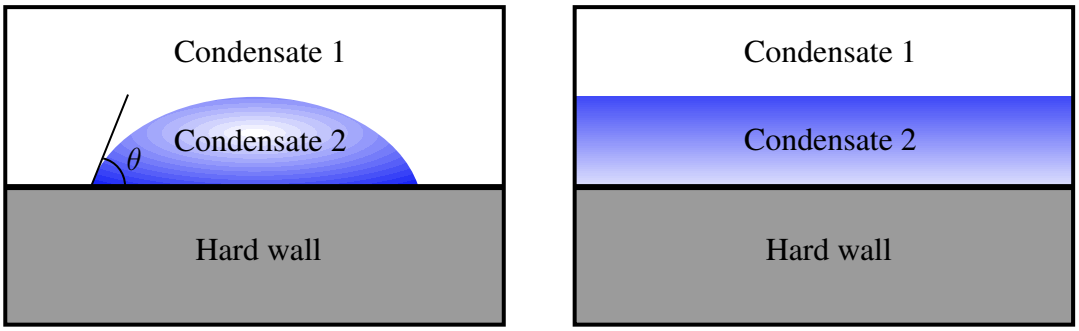

Figure 1. Illustration of the thermodynamic contact angle θ in the partial (left) and complete (right) wetting regimes of a binary Bose-Einstein condensate mixture

$$\gamma_1 = \gamma_2 + \gamma_{12}\cos\theta, \tag{2.1}$$

where θ represents the thermodynamic contact angle (see Figure1). Suppose that condensate 2 has a smaller surface free energy than condensate 1, i.e., $\gamma_2 < \gamma_1$. In this context, we are interested in the degree to which condensate 2 tends to wet the wall. The criterion for partial wetting is given by

$$\gamma_1 < \gamma_2 + \gamma_{12}, \tag{2.2}$$

while, in the case of complete wetting, where Youngs law is also referred to Antonovs law, the system reaches the thermodynamic limit in which

$$\gamma_1 = \gamma_2 + \gamma_{12}. \tag{2.3}$$

On the other hand, when $\gamma_1 < \gamma_2$, the roles of the two condensates are effectively reversed, prompting the question of how much condensate 1 tends to dry the wall. The distinction between wetting and drying in this context is purely conventional. This terminology is inspired by classical adsorption systems, where fluid 2 represents the liquid phase and fluid 1 its vapor. In the case of Bose-Einstein condensate mixtures, however, there is no fundamental physical difference between wetting and drying. Instead, the terminology serves as a useful indicator that when the contact angle $\theta > 90^\circ$, the labels assigned to condensates 1 and 2 switch their physical interpretation.

In this study, we investigate a static system consisting of a two-component Bose-Einstein condensate in prewetting phase, with condensate 1 always existing in the bulk phase at a constant density n_1. In contrast, condensate 2 is in contact with a particle reservoir, where the particle density can be adjusted so that the system reaches bulk phase equilibrium. From the pressure equilibrium condition $P_1 = P_2 = P$, with $P_j = g_{jj}n_j^2/2$, it is straightforward to obtain the equilibrium density of condensate 2 as

$n_2 = n_1\sqrt{g_{11}/g_{22}}$. Here, g_{ij} denotes the interaction constant characterizing the pairwise interaction between particles in condensates i and j, where $(i, j) = (1, 2)$. The condition for phase separation between the two components is $g_{12} > \sqrt{g_{11}g_{22}}$ [8]. Before the system reaches equilibrium, the density of condensate 2 is given by $\tilde{n}_2 = \epsilon n_2 < n_2$, with ϵ being a dimensionless scaling factor that quantifies the deviation of the density of condensate 2 from its equilibrium value (hereafter simply called the density ratio).

To determine the surface tensions at the wall (wall tensions), we consider the system in a semi-infinite space bounded by a hard wall at $z = 0$. This implies that the system of differential equations describing the condensate wavefunctions (the coupled Gross-Pitaevskii equations) reduces to a one-dimensional, time-independent system with respect to the spatial coordinate z

$$\begin{aligned} -\frac{\hbar^2}{2m_1}\frac{d^2\Psi_1}{dz^2} - \mu_1\Psi_1 + g_{11}\Psi_1^3 + g_{12}\Psi_2^2\Psi_1 = 0, \\ -\frac{\hbar^2}{2m_2}\frac{d^2\Psi_2}{dz^2} - \mu_2\Psi_2 + g_{22}\Psi_2^3 + g_{12}\Psi_1^2\Psi_2 = 0. \end{aligned} \tag{2.4}$$

where Ψ_i $(i = 1, 2)$ denotes the condensate wave function of species i. The hard wall at $z = 0$ leads to a Dirichlet boundary condition for the above system of equations as follows:

$$\begin{aligned} &\Psi_1(0) = \Psi_2(0) = \Psi_2(\infty) = 0, \\ &\Psi_1(\infty) = \sqrt{n_1}. \end{aligned} \tag{2.5}$$

Our goal in this work is to solve the coupled differential equations with the above boundary conditions in order to obtain analytical expressions for the condensate wavefunctions. These expressions allow us to compute the wall tension as well as the interfacial tension between the two condensates. Based on these surface and interfacial tensions, we further determine the thermodynamic contact angle via Youngs law. This angle characterizes the wetting behavior of one condensate on the wall in the presence of the other and plays a key role in the equilibrium morphology of the system.

2.2. Analytical expressions for the condensate wave functions

The coupled GP equations (2.4) are derived from the condition that the first variation of the grand potential Ω vanishes. The grand potential Ω, expanded to the lowest order in the fluctuation terms around the condensate wavefunction, is given by

$$\Omega = \int_V d\mathbf{r} \left(\sum_{i=1}^{2} \frac{\hbar^2}{2m_i} |\nabla\Psi_i|^2 + V_{\mathrm{GP}} \right), \tag{2.6}$$

with the GP potential density V_{GP} taking the form

$$V_{\mathrm{GP}} = \sum_{i=1}^{2} \left(-\mu_i |\Psi_i|^2 + \frac{g_{ii}}{2} |\Psi_i|^4 \right) + g_{12} \Psi_1^2 \Psi_2^2 \tag{2.7}$$

The GP potential density in Eq. (2.6) consists of three types of contributions. The terms $-\mu_i|\Psi_i|^2$ represent the energy associated with the chemical potential μ_i of each condensate component, where in the mean-field approximation one has $\mu_i = g_{ii} n_i$. The terms $g_{ii}|\Psi_i|^4/2$ account for the intraspecies interaction energy, with the factor of $1/2$ preventing double counting of particle pairs. Finally, the term $g_{12}|\Psi_1|^2|\Psi_2|^2$ describes the interspecies interaction energy between the two condensates.

It is evident that the quartic potential density in equation (2.7) leads to the nonlinear differential system (2.4), which does not admit exact analytical solutions. The approximation of a double-well potential by piecewise parabolic functions is mainly motivated by the advantage of working with segment-wise harmonic potentials. Such potentials make it possible to solve the equations of motion exactly in terms of simple functions with clear physical interpretation. Following this approach, we expand the quartic potential in (2.7) around its local minima, which correspond to the maxima of the condensate wavefunctions. Consequently, the GP potential density is replaced by a harmonic potential density as follows:

$$V_{\mathrm{DPA}} = \begin{cases} -P + (g_{12} n_1 - \mu_2) |\Psi_2|^2 + 2\mu_1 \left(\sqrt{n_1} - |\Psi_1| \right)^2, & \text{if } z > L, \\ -\epsilon^2 P + (g_{12} n_2 - \mu_1) |\Psi_1|^2 + 2\mu_2 \left(\sqrt{\epsilon n_2} - |\Psi_2| \right)^2, & \text{if } z < L, \end{cases} \tag{2.8}$$

where P is the equilibrium pressure. The approximation method we employ is known as the double-parabola approximation (DPA), which has been previously applied in several studies on static two-component BEC systems [2]-[6], as well as on three-component BEC systems [9]. The DPA is not a physically motivated approximation; rather, it is a purely mathematical simplification aimed at obtaining approximate analytical solutions of the GP equations. Previous studies have shown that although the wavefunction profiles derived from the DPA differ noticeably from those obtained numerically within the GP theory, the DPA still appears to capture the qualitatively correct interfacial structure. In particular, it provides a reasonable description of how the wavefunctions vary with the coupling constants.

By substituting the potential energy density in the grand potential (2.6) with the expression given in (2.8), and performing the variational procedure in the same manner as used to derive the system of differential equations (2.4), we obtain the following

approximate equations describing the condensate wavefunctions within the GP theory:

$$-\frac{\hbar^2}{2m_1}\frac{d^2\Psi_1}{dz^2}+2\mu_1\left(\sqrt{n_1}-\Psi_1\right)=0, \tag{2.9}$$

$$-\frac{\hbar^2}{2m_2}\frac{d^2\Psi_2}{dz^2}+\left(g_{12}n_1-\mu_2\right)\Psi_2=0,\ \text{if } z>L, \tag{2.10}$$

and

$$-\frac{\hbar^2}{2m_1}\frac{d^2\Psi_1}{dz^2}+\left(g_{12}n_2-\mu_1\right)\Psi_1=0, \tag{2.11}$$

$$-\frac{\hbar^2}{2m_2}\frac{d^2\Psi_2}{dz^2}+2\mu_2\left(\sqrt{\epsilon n_2}-\Psi_2\right)=0,\ \text{if } z<L. \tag{2.12}$$

Analytical solutions of Eqs. (2.9)-(2.12) take the following form:

$$\frac{\Psi_1(z)}{\sqrt{n_1}}=\begin{cases}1-A_1\exp\left(-\dfrac{\sqrt{4m_1g_{11}n_1}}{\hbar}z\right), & \text{if } z>L\\ 2A_2\sinh\left(\dfrac{\sqrt{2m_1g_{11}n_1(\epsilon K-1)}}{\hbar}z\right), & \text{if } z<L,\end{cases} \tag{2.13}$$

and

$$\frac{\Psi_2(z)}{\sqrt{n_2}}=\begin{cases}B_1\exp\left(-\dfrac{\sqrt{2m_2g_{22}n_2(K-\epsilon)}}{\hbar}z\right), & \text{if } z>L,\\ \sqrt{\epsilon}\left[1-\exp\left(-\dfrac{\sqrt{4\epsilon m_2g_{22}n_2}}{\hbar}z\right)\right]-2B_2\sinh\left(\dfrac{\sqrt{4\epsilon m_2g_{22}n_2}}{\hbar}z\right), & \text{if } z<L,\end{cases} \tag{2.14}$$

where

$$K=\frac{g_{12}n_2}{g_{11}n_1}=\frac{g_{12}n_1}{g_{22}n_2}=\frac{g_{12}}{\sqrt{g_{11}g_{22}}} \tag{2.15}$$

is known as the relative interaction parameter. As seen in Eqs. (2.13) and (2.14), it is convenient to introduce the auxiliary length scales

$$\xi_i=\frac{\hbar}{2m_ig_{ii}n_i},\ \text{with } i=(1,2). \tag{2.16}$$

From the continuity conditions of the wavefunctions and their first derivative at $z=L$,

the integration constants A_1, A_2, B_1, B_2 can be readily obtained as follows:

$$\begin{aligned}
A_1 &= \frac{\sqrt{\epsilon K-1}\exp\left(\sqrt{2}L/\xi_1\right)}{\sqrt{\epsilon K-1}+\sqrt{2}\tanh\left(\sqrt{\epsilon K-1}L/\xi_1\right)},\\
A_2 &= \frac{\operatorname{sech}\left(\sqrt{\epsilon K-1}L/\xi_1\right)}{\sqrt{2(\epsilon K-1)}+2\tanh\left(\sqrt{\epsilon K-1}L/\xi_1\right)},\\
B_1 &= \frac{\sqrt{2\epsilon}\exp\left(\sqrt{K-\epsilon}L/\xi_2\right)\left[1-\operatorname{sech}\left(\sqrt{2\epsilon}L/\xi_2\right)\right]}{\sqrt{2\epsilon}+\sqrt{K-\epsilon}\tanh\left(\sqrt{2\epsilon}L/\xi_2\right)},\\
B_2 &= \frac{\sqrt{\epsilon}\exp\left(-\sqrt{2\epsilon}L/\xi_2\right)\operatorname{sech}\left(\sqrt{2\epsilon}L/\xi_2\right)\left\{\sqrt{2\epsilon}+\sqrt{K-\epsilon}\left[\exp\left(\sqrt{2\epsilon}L/\xi_2\right)-1\right]\right\}}{2\sqrt{2\epsilon}+2\sqrt{K-\epsilon}\tanh\left(\sqrt{2\epsilon}L/\xi_2\right)}.
\end{aligned} \tag{2.17}$$

In the above expressions, L denotes the thickness of the prewetting layer. It is determined by the condition that the wavefunctions profiles intersect at $z = L$, i.e., $\Psi_1(L) = \Psi_2(L)$. Near the bulk two-phase coexistence, the thickness of the prewetting layer is obtained by solving this condition, which gives the following expression [4]

$$L = \frac{\xi_1}{2\sqrt{\epsilon K-1}}\ln\left(\frac{\sqrt{K-\epsilon}+\sqrt{2\epsilon}\,(1-\sqrt{\epsilon})+\epsilon\sqrt{\epsilon K-1}}{\sqrt{K-\epsilon}+\sqrt{2\epsilon}\,(1-\sqrt{\epsilon})-\epsilon\sqrt{\epsilon K-1}}\right). \tag{2.18}$$

2.3. Interfacial tension and thermodynamic contact angle

Since the system under consideration is semi-infinite with translational symmetry in the x-y plane, where the atoms are confined by a hard wall at $z = 0$, the grand potential (2.6) can be rewritten as

$$\Omega = A\int_0^\infty dz\left[\sum_{i=1}^{2}\frac{\hbar^2}{2m_i}\left(\frac{d\Psi_i}{dz}\right)^2+V_{\rm GP}\right], \tag{2.19}$$

where A is the area of the x-y surface.

Once the condensate wavefunctions have been determined, the next step is to compute the surface and interfacial tensions via the excess grand potential of the system. To compute the grand potential (2.19), we adopt a mechanical analogy similar to that presented in Ref. [10]. In this approach, the system of equations (2.4) takes the form of Newtons second law for a particle moving in a two-dimensional plane under the influence of a potential force. In this analogy, the mechanical energy of the particle is a conserved quantity and is given by

$$\sum_{i=1}^{2}\frac{\hbar^2}{2m_i}\left(\frac{d\Psi_i}{dz}\right)^2-V_{\rm GP}=\frac{g_{11}n_1^2}{2}=P. \tag{2.20}$$

By combining equations (2.19) and (2.20), we rewrite the grand potential of the system in the form

$$\Omega = A\int_0^\infty dz \sum_{i=1}^{2} \frac{\hbar^2}{m_i}\left(\frac{d\Psi_i}{dz}\right)^2 - PV. \tag{2.21}$$

On the right-hand side of Eq. (2.21), $\Omega_{\rm bulk} = -PV$ represents the bulk grand potential. The excess grand potential per unit area is referred to as the interfacial tension; therefore, we obtain

$$\gamma_{12} = \frac{\Omega - \Omega_{\rm bulk}}{A} = \int_0^\infty dz \sum_{i=1}^{2} \frac{\hbar^2}{m_i}\left(\frac{d\Psi_i}{dz}\right)^2. \tag{2.22}$$

Substituting (2.13) and (2.14) into (2.22) we obtain

$$\gamma_{12} = P(M\xi_1 + N\xi_2), \tag{2.23}$$

in which

$$\begin{aligned} M = {} & 2\sqrt{2}A_1^2 \exp\left(-2\sqrt{2}L/\xi_1\right) + 16B_2\left(B_2+\sqrt{\epsilon}\right)\epsilon L/\xi_1 \\ & + 4A_2^2\left[(\epsilon K-1)L/\xi_1 + \sqrt{\epsilon K-1}\sinh\left(2\sqrt{\epsilon K-1}L/\xi_1\right)\right], \end{aligned} \tag{2.24}$$

$$\begin{aligned} N = {} & 2B_1^2\sqrt{K-\epsilon}\exp\left(-2\sqrt{K-\epsilon}L/\xi_2\right) + 2\sqrt{2\epsilon}B_2^2\left[\exp\left(2\sqrt{2\epsilon}L/\xi_2\right) - 1\right] \\ & + 2\sqrt{2\epsilon}\left(B_2+\sqrt{\epsilon}\right)^2\left[1-\exp\left(-2\sqrt{2\epsilon}L/\xi_2\right)\right]. \end{aligned} \tag{2.25}$$

It can be readily confirmed that, as shown in Ref.[3], at bulk two-phase coexistence ($\epsilon = 1$), the coefficients M and N take the form

$$M = 2\sqrt{2}\frac{\sqrt{K-1}}{\sqrt{2}+\sqrt{K-1}}, \text{ and } N = \frac{4\left(1+\sqrt{2}\sqrt{K-1}\right)}{\sqrt{2}+\sqrt{K-1}}, \tag{2.26}$$

which subsequently leads to

$$\gamma_{12} = 2\sqrt{2}\frac{\sqrt{K-1}}{\sqrt{2}+\sqrt{K-1}}P(\xi_1+\xi_2) + 2\sqrt{2}P\xi_2. \tag{2.27}$$

Next, we determine the surface tension of a pure condensate j at the hard wall. For this purpose, we consider the half-space $z > 0$ filled exclusively with condensate j. In this case, Eqs.(2.9) and(2.12), combined with the hard-wall Dirichlet boundary condition at $z = 0$, yield the corresponding wavefunctions as

$$\Psi_1(z) = \sqrt{n_1}\left[1-\exp\left(-\sqrt{2}z/\xi_1\right)\right], \tag{2.28}$$

$$\Psi_2(z) = \sqrt{\epsilon n_2}\left[1-\exp\left(-\sqrt{2\epsilon}z/\xi_2\right)\right]. \tag{2.29}$$

The surface tension $\gamma_{i,\mathrm{pure}}$ is obtained by substituting Eqs. (2.28) and (2.29) and into Eq. (2.22). It can be readily seen that it scales linearly with ξ_i as follows:

$$\gamma_{1,\mathrm{pure}} = 2\sqrt{2}P\xi_1, \text{ and } \gamma_{2,\mathrm{pure}} = 2\sqrt{2}\epsilon^{3/2}P\xi_2. \tag{2.30}$$

Within the grand canonical ensemble, the excess grand potential per unit area has a unique definition up to an additive constant. In our setup, condensate 1 occupies the region above the interface, while condensate 2 is adsorbed onto the hard wall. Consequently, pure phase 1 dominates as $z \to \infty$. This excess quantity is calculated by taking the total grand potential Ω, subtracting the contribution from a half-space $(z > 0)$ entirely occupied by phase 1, and then dividing the result by the surface area parallel to the wall. Using the coupled GP equations (2.4), this leads to

$$\gamma_1 = \lim_{L\to\infty}\left[-\int_0^L dz\left(\frac{g_{11}}{2}\Psi_1^4 + \frac{g_{22}}{2}\Psi_2^4 + g_{12}\Psi_1^2\Psi_2^2\right) + P\int_0^L dz\right] \tag{2.31}$$

From Eq. (2.31), one can derive a relation between the surface tension of condensate 1 and the surface tensions in the pure phases,

$$\gamma_1 = \gamma_{1,\mathrm{pure}} + \gamma_{2,\mathrm{pure}} - \lim_{L\to\infty}\left(\int_0^L g_{12}\Psi_1^2\Psi_2^2 dz\right). \tag{2.32}$$

Near the bulk two-phase coexistence, the overlap term on the right-hand side of Eq. (21) is much smaller than the other two terms. Therefore, the surface tension of condensate 1 can be approximated as

$$\gamma_1 \approx \gamma_{1,\mathrm{pure}} + \gamma_{2,\mathrm{pure}}. \tag{2.33}$$

Substituting (2.23) and (2.33) into (2.1), we obtain the cosine of the thermodynamic contact angle,

$$\cos\theta = \frac{2\sqrt{2}}{M + N\xi_2/\xi_1}. \tag{2.34}$$

One can see that, in a bulk two-phase coexistence state with a stable contact angle θ, the value of $\cos\theta$ can be obtained by substituting M and N from Eq. (2.26) into the right-hand side of the above equation. Specifically,

$$\cos\theta = \left[\frac{\sqrt{K-1}}{\sqrt{2}+\sqrt{K-1}}\left(1 + \xi_2/\xi_1\right) + \xi_2/\xi_1\right]^{-1}. \tag{2.35}$$

Assuming that complete wetting is achieved at the end of the prewetting transition, this leads to a relation for K in terms of ξ_1 and ξ_2 as follows:

$$K = 1 + \frac{1}{2}\left(\xi_1/\xi_2 - 1\right)^2. \tag{2.36}$$

The curve representing the function $K(\xi_2/\xi_1)$, as shown in Figure 2, is referred to as the wetting phase boundary. This result has already been reported in Refs. [3] and [15]. However, what is important here is that it provides insight into suitable values of the relative interaction parameter K as a function of the ratio ξ_2/ξ_1, enabling the observation of variations in the contact angle throughout the prewetting phase, before it vanishes as the density ratio ϵ increases toward a certain value less than unity.

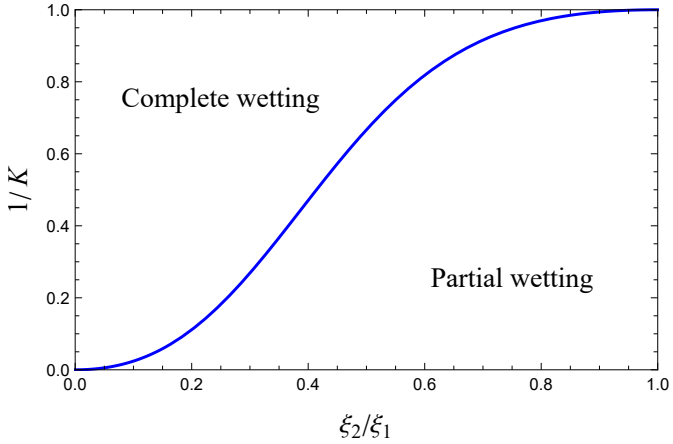

Figure 2. Wetting phase boundary in a binary BEC mixture adsorbed on a hard wall

Note that in our study, the contact angle varies as a function of the density ratio ϵ, and this dependence satisfies Eq. (2.34). Accordingly, for the case $\xi_1 = 2\xi_2$, Eq. (2.36) indicates that a prewetting transition occurs when the relative interaction parameter is chosen as $K = 1.3$. We would like to emphasize that the parameter K can be fully controlled in experiments via the Feshbach resonance technique [11]-[14].

As an illustration of Eq.(2.34), we plot the cosine of the thermodynamic contact angle as a function of the density ratio ϵ for the case $\xi_1 = 2\xi_2$ and $K = 1.3$ in Figure3. It can be seen that complete wetting is achieved before the bulk coexistence point is reached. In other words, the contact angle vanishes already at a density ratio $\epsilon < 1$, specifically at $\epsilon = 0.976$ in this figure, indicating the formation of a prewetting film with a finite thickness in the metastable regime. The thickness of this film then increases continuously and reaches macroscopic thickness as ϵ approaches 1. This behavior is consistent with a continuous (second-order) prewetting transition.

It is worth noting that although $\cos\theta$ approaches unity, this approach is not tangential. At first glance, such behavior may appear inconsistent with the typical characteristics of a second-order (continuous) wetting transition, in which $\cos\theta \to 1$ usually occurs smoothly and tangentially. However, as predicted in Ref. [1], this is not necessarily the case in systems where the interfacial potential barrier is absent and the grand potential exhibits near-degeneracy across a range of film thicknesses. In such cases, all intermediate film configurations are energetically comparable, allowing the

wetting film to grow continuously without requiring a vanishing slope in $\cos\theta$. Therefore, despite the finite-angle intersection with the line $\cos\theta = 1$, the prewetting transition remains second-order, characterized by the absence of a first-order jump in adsorption or film thickness.

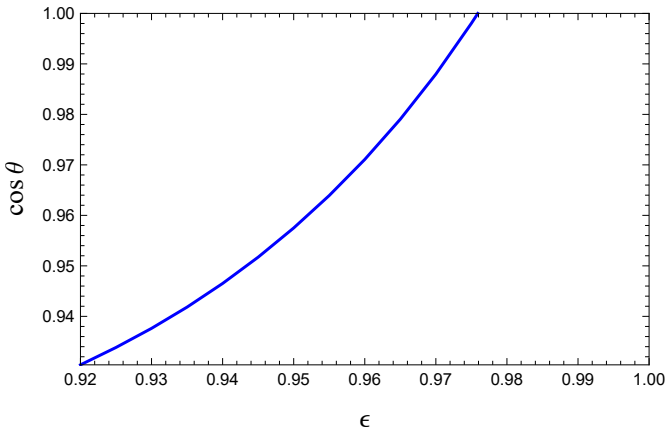

Figure 3. The cosine of the thermodynamic contact angle is plotted versus the density ratio ϵ ***for*** $\xi_1 = 2\xi_2$ ***and*** $K = 1.3$

3. Conclusions

In the foregoing sections, we have investigated the behavior of the thermodynamic contact angle in a binary Bose-Einstein condensate mixture adsorbed on a hard wall. By applying the double-parabola approximation, we derived an analytical expression for the thermodynamic contact angle. However, this expression remains algebraically intricate and cannot be reduced to a compact mathematical form. Encouragingly, our findings are in good agreement with the theoretical perspective presented in Ref. [1]. The prewetting transition exhibits a critical (second-order) nature, characterized by the absence of a discontinuous jump in film thickness between microscopic and macroscopic values. This is because the completely wetting state is established before the system reaches the bulk two-phase coexistence point. We hope that these results will offer valuable insights for experimentalists working with Bose-Einstein condensates to design and carry out potential verification experiments.

REFERENCES

[1] Indekeu JO & Van Schaeybroeck B, (2004). Extraordinary Wetting Phase Diagram for Mixtures of Bose-Einstein Condensates. *Physical Review Letters*, 93, 210402.

[2] Van Schaeybroeck B & Indekeu JO, (2015). Critical wetting, first-order wetting, and prewetting phase transitions in binary mixtures of Bose-Einstein condensates. *Physical Review A*, 91, 013626.

[3] Nguyen VT, (2016). Static properties of Bose-Einstein condensate mixtures in semi-infinite space. *Physics Letters A*, 380, 2920-2924.

[4] Pham DT & Nguyen VT, (2024). Static Properties of Prewetting Phase in Binary Mixtures of Bose-Einstein Condensates. *International Journal of Theoretical Physics*, 63(12), 315.

[5] Lo VT, Tran TTH, Vu VH, Chu GB, Nguyen QH, Tran KV, Dung LN, Le TL, Hoa DT, Nguyen TK & Pham TS, (2025). Interfaces movement in the segregated binary mixture of two weakly interacting Bose-Einstein condensates. *Annals of Physics*, 475, 169947.

[6] Pham DT & Dang TH, (2025). The interface position of a Bose-Einstein condensate mixture restricted by a hard wall in the double-parabola approximation. *Dalat University Journal of Science*, 15(3S), 33-43.

[7] Rowlinson JS & Widom B, (2013). *Molecular Theory of Capillarity*. Courier Corporation.

[8] Ao P & Chui ST, (1998). Binary Bose-Einstein condensate mixtures in weakly and strongly segregated phases. *Physical Review A*, 58(6), 4836-4840.

[9] Indekeu JO, Nguyen VT & Jonas Berx, (2025). Three-component Bose-Einstein condensates and wetting without walls. *Physical Review A*, 111, 043320.

[10] Pham DT, Tran KV & Nguyen VT, (2025). Phenomenological analogy between Gross-Pitaveskii theory for Bose-Einstein condensate mixtures in infinite space and Classical mechanics. *HNUE Journal of science: Natural Science*, 70(1), 25-35.

[11] Inouye S, Andrews MR, Stenger J, Miesner HJ, Stamper-Kurn DM & Ketterle W, (1998). Observation of Feshbach resonances in a Bose-Einstein condensate. *Nature*, 392(6672), 151-154.

[12] Stan CA, Zwierlein MW, Schunck CH, Raupach SMF & Ketterle W, (2004). Observation of Feshbach resonances between two different atomic species. *Physical Review Letters*, 93(14), 143001.

[13] Papp SB & Wieman CE, (2006). Observation of Heteronuclear Feshbach Molecules from a Rb 85-Rb 87 Gas. *Physical Review Letters*, 97(18), 180404.

[14] Chin C, Grimm R, Julienne P & Tiesinga E, (2010). Feshbach resonances in ultracold gases. *Reviews of Modern Physics*, 82(2), 1225-1286.

[15] Indekeu JO, Lin CY, Nguyen VT, Van Schaeybroeck B & Tran HP, (2015). Static interfacial properties of Bose-Einstein-condensate mixtures. *Physical Review A*, 91, 033615.